



MINISTRY OF AVIATION

AERONAUTICAL RESEARCH COUNCIL
REPORTS AND MEMORANDA

Some Notes on the Flow Patterns
Observed over Various Swept-back
Wings at Low Mach Numbers
(in the R.A.E. 10-ft \times 7-ft High
Speed Tunnel)

By

A. B. HAINES, B.Sc.

© Crown Copyright 1960

LONDON: HER MAJESTY'S STATIONERY OFFICE

1960

NINE SHILLINGS NET

Some Notes on the Flow Patterns Observed over Various Swept-back Wings at Low Mach Numbers (in the R.A.E. 10-ft × 7-ft High Speed Tunnel)

By

A. B. HAINES, B.Sc.

COMMUNICATED BY THE PRINCIPAL DIRECTOR OF SCIENTIFIC RESEARCH (AIR)
MINISTRY OF SUPPLY

*Reports and Memoranda No. 3192**

September, 1954

Summary.—This paper collects together the flow patterns observed by an oil film (titanium oxide) technique over ten different swept-back wings at high incidence and low Mach number in the Royal Aircraft Establishment 10-ft × 7-ft High Speed Tunnel. The designs range from 0·04 to 0·10 in mean thickness/chord ratio and from 40 deg to 60 deg in angle of sweep. Almost all the wings suffer from a leading-edge separation and the paper discusses in general terms how the regions of flow separation, together with their associated part-span vortex sheets are affected by changes in incidence, Reynolds number and wing design. Some brief reference is made to how the flow patterns are related to the overall force and moment characteristics and how these characteristics might be improved by the use of different types of modification.

It appears that some correlation may ultimately be established between the spanwise extent of the separation over a swept-back wing at a given incidence with concepts based on two-dimensional flow and the pressure distribution over the swept wing in potential flow. No correlation can be expected in terms of the chordwise extent of the separation, in view of the presence of 'part-span vortex sheets'. The need for research into the 'bursting' of 'short' separation bubbles in two-dimensional flow and into the nature and reasons for the part-span vortex sheets in three-dimensional flow is especially emphasized.

1. *Introduction.*—The flow over the surface of various swept-back wings at high incidence and low Mach number has been studied in the R.A.E. 10-ft × 7-ft High Speed Tunnel by an oil-film technique with a view to obtaining a better understanding of the stalling characteristics of such wings. The flow patterns for each individual wing and the correlation between them and the measured overall forces and moments are given in other reports (e.g. Ref. 1). It was thought to be desirable, however, also to collect together into one document, a representative selection of the photographs that have been obtained. This is done in the present paper. No attempt is made here to discuss the results in close quantitative detail. Instead, the emphasis here is on the basic qualitative features and in showing where these recur from one wing to another and where there are differences in behaviour. Not all the observed features can be interpreted with certainty; in some cases, tentative explanations are advanced in order to stimulate discussion.

A full description of the technique used for visualizing the flow is included in Ref. 1. The model wings are coated with a suspension of titanium oxide in light diesel oil with a little oleic

* R.A.E. Tech. Note Aero. 2330, received 13th November, 1954.

TABLE
Details of Wing Designs

Wing	Angle of sweep (deg)	Aspect ratio	Taper ratio	Thickness-Chord Root-Tip	Maximum-thickness position (also section shape) Root/Tip	Remarks	R for flow photographs $\times 10^6$	Photographs in Figures
A	40 (0.25c)	3.5	0.40	0.06	0.31c (RAE 101)	—	1.1, 1.9, 2.8, 5.7	1, 2, 3a (see also Fig. 1)
B	48.6 (0.25c)	3.2	0.38	0.075	0.38c	Also tested with wing-root intake; results for clean wing given in Ref. 1	2.5, 6.0	3b, 4
C	50 (0.25c)	3.1	0.36	0.075	0.31c (RAE 101)	3 tests: (i) Basic wing (Ref. 1) (ii) With fence at 0.56 \times semi-span (Ref. 1) (iii) With drooped nose (Fig. 10) outboard of 0.56 \times semi-span	2.7	8, 9
D	60 (L.E.)	2.0	0.073	0.04	0.30c	Wing-root intake with sharp upper lips	2.7	5
E	49.9 (L.E.) (except for wing-root fillet)	3.2	0	0.136/0.10/0.08 (0.10 at 0.34 \times semi-span)	0.15c/0.30c/0.31c (NACA 0010 at 0.34 \times semi-span. RAE 101 shape at tip)	Root fillet with 65 deg of sweep on the leading edge and with a thickness/chord ratio of about 0.136 throughout	2.3	6
F	40 (0.25c)	3.5	0.40	0.10	0.15c/0.50c	Section shape varying span-wise from bluff-nosed root section with $\rho_{L.E.} = 0.033c$ to sharp-nosed tip section with $\rho_{L.E.} = 0.0018c$	2.0	7

acid added to act as a dispersion agent. After starting the fan, the oil flows over the surface and eventually dries off or is blown off, leaving the flow pattern recorded in the titanium oxide which is left deposited on the wing. Since the oil flows under the action of various types of forces, care is needed in interpreting the flow patterns in order to distinguish between those features that can be regarded as truly representative of the airflow over the wing and those that are merely a consequence of the tendency of the oil, under certain circumstances, to flow towards or circulate around the peak-suction positions on the wing. In the latter case, the behaviour of the oil can still be used as a guide to the nature of the pressure distributions over the wing surface. To interpret the patterns successfully, it is best to consider not merely the final pictures taken after the oil has dried but also the manner in which these patterns have developed. This is preferably done by actual observation but to meet this point in the present paper, a proportion of the photographs reproduced were taken while the oil was still wet and flowing over the wing surface (*e.g.*, all except that for $\alpha = 8$ deg in Fig. 1).

2. *Range of Wing Designs Tested.*—Broadly speaking, the flow patterns that have been obtained are for wings with angles of sweep of from 40 deg to 60 deg and with thickness/chord ratios varying from 0.04 to near 0.10. Their principal geometric features are listed in the Table on page 2.

Many of the more important flow characteristics that are common to several of the wings tested can be seen clearly in the photographs for Wing A and so, particularly as photographs are available in this case for four different Reynolds numbers between $R = 1 \times 10^6$ and $R = 6 \times 10^6$, it is convenient to treat this wing as the basic example. Wings A and B are of what may be termed 'simple' design in that they have the same section shape and thickness/chord ratio at all stations from root to tip, no 'kinks' or discontinuities in plan-form, no twist and no complicating features such as a wing-root intake fairing. Qualitatively, the flow patterns observed for these three wings are similar to those observed on several other wings with thickness/chord ratios between 0.04 and 0.08 and similar amounts of sweep. Wing A has 6 per cent thick sections and 40 deg sweep; Wing B has 7.5 per cent thick sections and 50 deg sweep.

Wing D is included for two reasons. First, the comparison between Wings A, B and D is useful in showing how the flow patterns at the Reynolds numbers of these tests are affected by an increase in sweep to 60 deg and a decrease in thickness/chord ratio from 0.06 to 0.04. Second, the flow patterns over Wing D at high incidence are influenced appreciably by the presence of the wing-root intake, which has sharp upper lips; for this reason, Wing D does not quite fall within the category of 'simple' wings, as defined above.

The remaining examples all possess some complicating design feature. With Wings E and F the section shape varies from a blunt-nosed section with a far forward position for the maximum thickness at the root to a relatively sharper-nosed section at the tip. In the case of Wing E, this variation is not important in the present context because most of the variation is confined to the sections close to the root and in the incidence range of the present tests, the flow does not separate over these sections. Wing E is of interest more particularly because even near the tip, its leading-edge radius* is larger than for any of the other wings considered here and it is found that this is the only wing of the present collection where the separation over the outer sections is thought to be a turbulent separation from the rear. The results for this wing are therefore perhaps more akin to those which might be expected with thicker wings of comparable sweep at similar Reynolds numbers or also with several more of the present wings at the Reynolds numbers of flight. The results for Wing F, on the other hand, are of interest here because they illustrate how the flow patterns are affected by a spanwise variation in the leading-edge radius of the outer sections.

Finally, the photographs in Figs. 8 and 9 for design C are included to illustrate two of the ways in which both the flow and the overall force and moment characteristics of such a swept-back

* In terms of the local chord.

wing at high incidence can be improved. The basic wing¹ is closely similar, except for a different section shape, to Wing B and consequently, the flow patterns are also qualitatively similar. Photographs are included to show the effects of fitting a full-chord fence¹ at $0.56 \times$ semi-span or alternatively, of modifying the leading-edge shape of the wing, outboard of this station. The modified nose shape is known in Fig. 10; it involves both some camber and some local thickening and, in order to fair into the original shape as quickly as possible behind the leading edge, this is extended forward by $0.025c$. The inner end of the modification at $0.56 \times$ gross semi-span is discontinuous.

Two points about the experiments need to be mentioned. First, the tests on Wings D and E were made on complete, sting-supported models for which the maximum available incidence was about $\alpha = 13$ deg. Hence, in these cases, it was not possible to investigate the stalling characteristics fully, e.g., $C_{L \max}$ could not be reached. The other wings were half-models and generally, unless the models vibrated too severely, it was possible to reach $\alpha = 22$ deg. The second point concerns the half-model technique. All the half-models (A, B, C and F) were tested with the half-wing mounted on the balance plate and with the half-fuselage mounted separately on the floor of the tunnel, leaving a gap in the wing-body junction. Flow through this gap into or out of the dead space surrounding the working-section of the tunnel was prevented by a mercury seal but there was still some flow over the wing stub above the seal. The general direction of this flow is downward near the wing leading edge and outward further back so that its chief effect on the observed flow patterns is to impart an appreciable outward spanwise component to the oil flow over the rear of the inboard sections at high incidence (for reasons of stub design, the effect is relatively minor in the case of Wing F). A few tests made with the gap in the wing-body junction specially sealed, showed that the deviation from the free-stream direction of the oil flow near the root of Wings A, B and C could be at least doubled by this spurious effect present when the gap is open. On the other hand, these comparative tests suggested that the extent of the region of separated flow and the positions of any part-span vortex sheets further out on the wing were not significantly influenced by this effect and so the flow patterns, as presented here, should not be misleading in their more important respects.

3. *Discussion of Flow Characteristics at High Incidence.*—3.1. *General Survey of Changes with Increasing Incidence.*—All the wings considered here, except probably Wing E, which is effectively thicker than the rest, have one feature in common: the flow separation at high incidence is of a 'leading-edge' type² except possibly for the sections close to the root, where a turbulent separation from the rear may occur first.

As the incidence is increased, the flow separates first near the tip or, at least, at a position further out along the span than the position for the maximum in the spanwise distribution of C_L . There are two principal reasons for this:

- (i) The spanwise variation in the shape of the chordwise loading: near mid-semi-span, the chordwise loading is similar in shape to that on an aerofoil in two-dimensional flow but near the tip the loading is distorted so that the peak suction on the upper surface for a given local C_L is both greater in magnitude and occurs nearer the leading edge. Both effects would increase the risk of the boundary-layer separating, particularly at low Reynolds numbers.
- (ii) The taper of the wings implies that the local Reynolds number (R_l), based on the local chord, is smaller near the tip. This is an important factor in those cases in which the local C_L , $C_{L \text{ crit}}$, at which separation first occurs, is varying rapidly with Reynolds number (e.g., Wing A at $R_{\text{mean}} = 2.8 \times 10^6$; see Fig. 11).

A typical flow pattern for a case where the flow has only separated over part of the span is the pattern for Wing A at $\alpha = 9$ deg, $R = 2.8 \times 10^6$ (Fig. 1). The photograph for this condition, included in Fig. 1, was taken before all the oil had dried and crudely speaking, the upper wing surface can be divided into three distinct regions: First, that over the forward part of the outer

sections where no oil flow has yet taken place and hence where there can be little airflow close to the surface; second, inboard and to the rear of this substantially dead-air region, there is an area where there has been very rapid scouring by the oil, leaving a herring-bone effect and third, inboard of this again, where the only significant effect is the spanwise drift of the sub-layer in the boundary layer. By comparing the 'early' and 'late' photographs for $\alpha = 18$ in Fig. 3a, it will be observed that a flow pattern is subsequently produced over what has been termed the 'substantially dead-air region' by oil from further inboard turning and flowing forward over this region but the rate of this flow is very slow and its existence does not affect the basic contention (see also Section 3.2.1).

The herring-bone pattern has been taken to indicate the presence of a 'part-span vortex sheet', originating from near the leading edge near the inboard end of the separation. It can be thought of as a sheet of trailing vortices arising from the bound vortices on the inner part of the wing that do not carry on into the separated region. The term 'part-span' signifies that the vortex sheet occurs somewhere along the span and not necessarily near the tip. By referring to it as a 'vortex sheet', this is not intended to preclude the possibility that the effects observed in the surface flow pattern are associated with a sheet that has already rolled up to give the impression of a core of vorticity. More evidence is required both on this point and on the precise mechanism controlling the formation of the sheet. This last point is referred to again in Section 3.2 but meanwhile, it can be suggested that the approximate location of the projection of the vortex sheet in the wing surface is given by the locus joining the points at which the oil flow lines in the forward part of the herring-bone pattern have diverged most (outward) from the free-stream direction. The forward part of the pattern represents therefore flow under the vortex sheet while the 'backbone' marks a 'line of reattachment' behind which there is again 'attached' and predominantly streamwise flow which has come over the top of the sheet. Indeed, the flow behind this line and in the region influenced by the sheet is more nearly in the free-stream direction than is the flow nearer the wing-root. This may be largely because the sheet itself will impart an inward component to the flow over the top, corresponding to the outward component underneath it but other factors that may contribute to the observed pattern are first, effectively, a new relatively thin boundary layer starts behind the line of reattachment and second, since air is being entrained from out in the free stream, it is not subject to the spanwise component induced by the flow through the gap in the wing-body junction.

One of the most significant characteristics is the shape of the projection of the vortex sheet in the wing surface. The photographs show that the vortex sheet is always diverted out, relative to the free-stream direction. In many cases, the angle in question amounts to about 20 deg over much of the chord. Towards the trailing edge of the wing, the vortex sheet sometimes bends back towards the free-stream direction. It is found that the approximate figure of 20 deg applies equally well for wings of widely differing angles of sweepback, as can be seen by comparing the directions of the vortex sheets over Wings A, B and C (Figs. 1 to 5 and Fig. 8). At low Reynolds numbers and particularly for the thinner wings, the angle tends to be greater than 20 deg for moderate incidences, *i.e.*, the vortex sheet then tends to lie in a direction only slightly inclined to the leading edge of the wing (*e.g.*, *cf.* Figs. 1 and 2). This is another point to which we shall return in Section 3.2.

With increase in incidence, the inboard end of the separation and hence the origin of the vortex sheet approach the wing-root leading edge but this movement becomes very slow when the separation has already extended to close to the wing root. In other words, the flow near the wing-root leading edge does not separate until the local C_L there has reached an appreciably higher value ($C_{L \text{ crit}}$) than is required for separation near the leading edge on the sections further out on the wing. The detailed analysis of the flow patterns for Wing A, for example, shows that for this wing, the values of $C_{L \text{ crit}}$ for the sections within about 0.1 of the semi-span of the wing root are at least about 0.2 higher than for the sections near mid-semi-span, assuming the same value for the local Reynolds number (Fig. 11). The reason for this delay in the separation near the wing-root leading edge is, of course, the same as the principal reason for the premature

separation near the leading edge near the tip: near the root of a swept-back wing, the chordwise loading is modified so that the peak suction on the upper surface for a given local C_L is smaller and further back from the leading edge than for the sections further outboard.

Hence, at high incidence, a vortex sheet continues apparently to originate from near the same point near the wing-root leading edge over quite an appreciable range of incidence. It may be noted that even when the separation does extend fully into the side of the body, a vortex sheet may still be expected here because the flow over the body may still remain attached. Since the vortex sheet effectively forms the inner lateral boundary of the separated region and in view of the characteristic shape adopted by the projection of the vortex sheet in plan view, it follows that, whereas near the leading edge the inward extension of the separation with incidence tends to be halted close to the wing root, for positions further back along the chord, it is halted further out on the span. Strictly, to understand the behaviour of the flow correctly, one should think in terms of the direction of the local stream but, nevertheless, it is convenient to draw conclusions regarding the extent of the separated region in the free-stream direction. This is certainly preferable for visualizing how the growth of the separation is likely to affect the overall forces and moments. In this context, therefore, it can be said that when the inward extension of the separation becomes very slow, the presence of the part-span vortex sheet effectively limits the rearward extension (in the free-stream direction) of the dead-air region over the sections for a little way outboard of the origin of the sheet. This effect has been observed both when the separation, as above, has extended to near the wing-root leading edge and also in examples where a fence has been fitted round the leading edge of a wing at some point along the span and when the separation has extended from the tip to near the outer side of the fence (Wing C, Fig. 8). In extreme cases, it has even been found that over a small range of incidence, the dead-air region over the outer sections may decrease in chordwise extent with increasing incidence. This occurs when the increase in incidence has little effect on the actual position of the sheet (as previously defined) but increases its strength so that there is an increase, both forward and rearward, in the area over the wing surface over which there is a strong spanwise flow. This effect can be observed, for example, with Wing D by comparing the photographs for $\alpha = 10.5$ deg and $\alpha = 12.6$ deg in Fig. 5.

As the incidence is increased further, the next qualitative change that occurs is usually not that the part-span vortex sheet disappears but rather that it appears to lift off the surface and the chordwise position at which this happens moves forward from near the trailing edge, as the incidence is increased (This can be seen most clearly in the photographs for $\alpha = 18, 20$ and 22 deg for Wing C with its drooped nose modification (Fig. 9)). In the general case, the proportion of the span over which the dead-air region close to the surface extends over the whole chord aft of the point of separation then progressively spreads inward. $C_{L\max}$ for the wing as a whole is usually attained at some stage in this process. The apparent lifting of the vortex away from the surface of the wing, except possibly close to the leading edge, can be explained in various ways and the same explanation may not hold for every example. Possible lines of thought are as follows:

- (i) So far, we have merely considered the surface flow patterns. Ref. 3, however, reports on some tests in which measurements were made of the pressures not merely on the surface but also in the flow field around a delta wing at high incidence. These showed that in the neighbourhood of what we have so far called a part-span vortex sheet, the suctions are increased most near a line whose projection in the wing surface is similar to the line we have so far taken as defining the position of a part-span vortex sheet, but in side elevation, the distance between this line and the wing surface steadily increases with distance back from the leading to the trailing edge. This might have been expected for even a vortex sheet that has not rolled up since the vorticity would tend to be concentrated near the top of the sheet. It follows that the influence of the vortex sheet on the surface pressure distribution should decrease towards the trailing edge. Ultimately, at high incidence, it should become slight when and if the effect of the increasing displacement between the more important part of the sheet and

the wing surface more than outweighs the effects caused by the increase with incidence in the strength of the sheet. It may be noted, incidentally, that despite this decrease in the sphere of influence on the wing surface, the influence of the vortex sheet on the general flow field and, in particular, on the downwash behind the wing should continue to increase with incidence.

- (ii) If, on the other hand, the sheet has already rolled up above the wing surface and not merely aft of the trailing edge, the line referred to above as joining the points for the maximum increase of suction probably represents the axis about which the sheet rolls up and it is easy to visualize that at some point the rolled-up vortex will break clear from the wing surface. It is pertinent to note that the sheet should tend to roll up more rapidly, the greater its vorticity.
- (iii) Much of what is observed in the oil-flow patterns may simply be a result of the increased spanwise drift of the sub-layer of the boundary layer over the inner wing at high incidence. This is certainly true, for example, of the flow patterns for Wing A at $\alpha = 18$ deg, $R = 3 \times 10^6$ (Fig. 3a). From the relative rates of oil flow over different parts of the wing, it appears that the vortex sheet is still influencing the surface flow pattern back to near the trailing edge but aft of about $0.5c$. It is likely that the direction of the oil-flow lines is being principally determined by the spanwise drift of the relatively thick boundary layer.
- (iv) Finally, in some cases a turbulent separation near the rear of the root sections may occur and eventually there may be no attached boundary layer aft of the vortex sheet.

The chief exceptions to the above general description of how the flow patterns develop with increasing incidence are Wings E, F and C, with its special droop-nose modification. Wing E behaves as an effectively thicker wing*: separation again occurs initially far out on the wing but is thought to be a turbulent separation from the rear at the test Reynolds number†. With this design, the dividing line between the parts of the wing where the flow has or has not separated lies more nearly in the free-stream direction and the vortex sheet between the two regions appears to be much weaker; at least, in its effects on the surface flow patterns (Fig. 6). The white 'blob' about which the oil-flow lines tend to rotate is thought to mark the approximate position of the peak suction on the wing, *i.e.*, outboard of it, there is a reduction in the circulation as a result of the separation (Fig. 6).

The flow pattern for Wing F at $\alpha = 10$ deg, $R = 2 \times 10^6$ (Fig. 7), when the separation is confined to near the tip where the leading-edge radius is relatively sharp, is similar to the general type, as observed for Wings A and B. At higher incidences, however, when the separation has extended further inboard to where the leading-edge radius is greater, the patterns become similar to those observed on Wing E (*see above*). This can be seen particularly from the photographs for $\alpha = 14$ deg, 18 deg in Fig. 7. Wing F is therefore a most interesting example in which the two types of behaviour can both be observed.

Wing C with its drooped nose is discussed in Section 4 and Ref. 4.

The chief omissions in the description so far that need some more detailed comment are the nature of the outboard separation, the inter-relation between the growth of the separation and the influence of the vortex sheet and the effects of changes in Reynolds number. These are now discussed in Section 3.2.

3.2. Detailed Discussion (Including the Nature of the Separation and the Effects of Changes in Reynolds Number).—It is convenient here to digress and consider what happens in two-dimensional flow when the aerofoil is sufficiently thin and the Reynolds number sufficiently low

* It may be noted that in Section 3.2, it will be suggested that the effective section is one intermediate between those in the free-stream direction and perpendicular to the leading edge.

† Pressure-plotting tests on a wing of closely similar design have confirmed that this is certainly true for $M = 0.5$.

for the stall to be caused by a separation of the laminar boundary layer from close to the leading edge. Usually, the laminar layer first separates at some incidence well below that for $C_{L \max}$ but two types of stall can be distinguished, according to how this separation varies with increasing incidence. In the first type, which has been studied in detail², for example, with a 9 per cent thick section at $R = 6 \times 10^6$, for all incidences until just less than that for $C_{L \max}$, the separated boundary layer continues to reattach as a turbulent layer soon behind the point of separation. The chordwise extent of the 'short' bubble so formed actually decreases with increasing incidence in this range and the pressure distribution over the surface is hardly affected by its presence. $C_{L \max}$ occurs when the separated layer suddenly fails to reattach or the bubble 'bursts'. In the second type of leading-edge stall, found, for example, with a 6 per cent thick, NACA 64 series section at $R = 6 \times 10^6$ (see Ref. 2), the chordwise extent of the separation bubble steadily increases with increasing incidence from the incidence at which it first appears. Its length throughout is of a completely different order of magnitude from that of the 'short' bubble above. With such a 'long' bubble type of separation, the forces and moments are affected significantly at incidences less than that for $C_{L \max}$, e.g., the lift-curve slope is reduced and there is a rearward movement of the aerodynamic centre. Even at the incidence for $C_{L \max}$, the flow over the upper surface is probably still reattaching somewhere ahead of the trailing edge. The question as to which type of bubble is to be expected on a given section at a given Reynolds number is related to the difference between the chordwise positions at which the laminar layer separates and at which a transition to turbulence occurs. A criterion has been suggested⁴, based on the local Reynolds number (R_{δ^*}) at the point of separation, using the local boundary-layer displacement thickness (δ^*) as the representative length. A long bubble should result if $R_{\delta^*} <$ about 400. It follows that a long bubble is more likely with a thin section. Expressed another way, for a given section, at a very low free-stream Reynolds number, it is likely that a long bubble will form almost immediately after the incidence has increased to a value sufficient to give a peak suction near the leading edge on the upper surface. With increasing Reynolds number the incidence or value of C_L at which a long bubble first forms should increase until, ultimately, a long bubble does not form at all, *i.e.*, the stall has either reverted to the first type in which a short bubble bursts before a long bubble can form or possibly it may even change to being caused by a turbulent separation further aft. The Reynolds number for the disappearance of the long bubble increases as the thickness/chord ratio, or more strictly, the leading-edge radius is reduced. In the extreme case of a sharp-edged plate, a long bubble should always form, whatever the Reynolds number.

Reverting to the swept-back wing, it is certainly clear that the leading-edge separation that has been mentioned as starting near the tip and extending inward and rearward with increasing incidence is not a mere 'short' bubble (at lower incidences or inboard of the part-span vortex sheet, a short bubble may, however, be present and a close examination of the flow patterns has suggested that this is often so, even at zero incidence at the Reynolds numbers of these tests). It is, however, more difficult to decide whether the outer separation is analogous with a 'long' bubble or with a 'burst short' bubble. This is particularly so because it appears doubtful whether the distinction, applicable in two-dimensional flow (that in one case, the separated layer reattaches within the wing chord and in the other case, it does not), can be carried over to the three-dimensional problem. No positive evidence has been found in any flow photograph of the flow reattaching *via* a transition to turbulence in the region on the wing outboard and ahead (in a free-stream sense) of the vortex sheet. It must be added, however, that this cannot be regarded as conclusive evidence that such a reattachment does not in fact occur. A reattachment *via* a transition to turbulence would be difficult to detect from merely an oil-flow pattern because even if no part-span vortex sheet were present, there would be a slow motion of the oil both spanwise and forward within the bubble, while after reattachment the oil close to the surface would have a strong spanwise velocity component*. Even if reattachment in this region does in fact occur, it is unlikely that there is any close correlation between the growth with incidence of the extent of

* Even in two-dimensional flow, the line of reattachment behind a long bubble would appear in an oil pattern as a somewhat confused region with slow forward motion ahead and orderly flow behind it,

the bubble on the swept wing, measured along the direction of the local stream with that on some corresponding section in two-dimensional flow. This is partly because the pressure within a three-dimensional bubble is not the same as with a two-dimensional bubble of the same cross-sectional shape and partly because the vortex sheet induces cross-flows which, themselves, would be expected to deform the shape of the bubble. Whatever the uncertainties regarding the possible length of the bubble in the direction of the local stream, it can be definitely concluded that there can be no precise correlation between the growth with incidence of the chordwise extent (*i.e.*, in the free-stream direction) of the dead-air region over the swept wing and of the bubble over some effectively corresponding section in two-dimensional flow. Over an appreciable length of the span, outboard of the origin of the vortex sheet, the rearward boundary of the dead-air region and the line of reattachment on the swept wing (thinking in terms of the free-stream direction) are dictated by the position and velocity components induced by the part-span vortex sheet, for which there is no parallel in the two-dimensional case. Although there is no precise correlation, it will be seen later that the shape of the projection of the vortex sheet in the wing surface and nature of the outboard separation are mutually dependent, at least, under certain conditions.

To return to the discussion of the actual mechanism of the leading-edge separation, another way of expressing the distinction between a 'long' and a 'burst short' bubble is to say that with the first but not the second type, a significant separation first occurs at a value of C_L that is notably less than the local $C_{L \max}$ and that varies appreciably with the local Reynolds number (unless the Reynolds number is very low indeed). On this basis, it is possible to establish a correlation between the swept wing and the two-dimensional aerofoil by making a quantitative analysis of the flow patterns over the swept wing, particularly if these are available as for Wings A and B, at more than one free-stream Reynolds number. From the photograph for a given incidence, the spanwise position for the inboard end of the significant separation can be roughly determined; the local C_L at this position can be estimated approximately* and so a plot can be constructed, as in Fig. 11 for Wing A, relating the local C_L ($C_{L \text{ crit}}$) at which the flow first separates with the Reynolds number (R_l), based on the local chord. The figures against the points denote the appropriate positions along the span. The values of C_L are reduced for sections near the tip and increased for sections near the root, as previously explained, but it is possible to draw a mean curve for sections over the central portion of the semi-span, *e.g.*, from about $\eta = 0.2$ to 0.75 . Although the result may be in error quantitatively, it seems certain that the variation of $C_{L \text{ crit}}$ with R_l is substantially of the form shown and hence is qualitatively similar to what might be expected in two-dimensional flow. Up to some value of the Reynolds number, the value of $C_{L \text{ crit}}$ is sensibly less than the local $C_{L \max}$ and is varying appreciably with R_l : in this range, the conditions determining the value of C_L at which the flow separates and the shape of the bubble, close to the leading edge and well away from the vortex sheet should bear some analogy to the case of a long bubble in two-dimensional flow. At higher Reynolds numbers, there should be a correspondence with conditions for a short bubble to burst; at these Reynolds numbers, the flow would not reattach further aft along the chord, if it were not for the rotary effect introduced by the vortex sheet.

A quantitative analysis, such as that for Fig. 11 has been made for Wings A, B and C (unmodified) with the results that the changeover from one type of leading-edge stall to the other appears to occur† at about

$$R_l \simeq 5.5 \times 10^6 \text{ for wing A (6 per cent, RAE 101, } \phi = 40 \text{ deg)}$$

$$R_l \simeq 4 \times 10^6 \text{ for wing C (7.5 per cent, RAE 101, } \phi = 50 \text{ deg)}$$

$$R_l \simeq 5.5 \times 10^6 \text{ for wing B (7.5 per cent, } \rho_{LE} \text{ effectively smaller}^1 \\ \text{than for RAE 101 section,} \\ \phi = 48.6 \text{ deg).}$$

* No allowance has been made for non-linear effects and in particular, the effects of a part-span vortex sheet on the spanwise loading inboard of it have not been considered. Hence the local values of C_L are underestimated by an amount that is greatest for the sections near the root of the wing.

† Excluding sections near the tip and root of the wing.

These values suggest that the same trends with thickness/chord ratio and leading-edge radius apply as in two-dimensional flow but the angle of sweep (presumably of the leading edge) also exercises a quantitative influence. It seems that the Reynolds number above which a 'quasi-long' bubble does not form decreases with increasing sweep for a given section in the free-stream direction (Supporting evidence for this is that the separation at $R = 6 \times 10^6$ for a 6 per cent thick section with a shape not too dissimilar from that of Wing A is still definitely of the long-bubble type in two-dimensional flow²). In other words, in any attempt at correlating the behaviour of wings with different angles of sweep, the effective section on the swept wing is inclined to the free-stream direction, although probably not so much as to be perpendicular to the leading edge.

The above values also suggest that for all wings with thickness/chord ratios of 0.06 or more, and possibly for quite a number of thinner wings, the separation at incidence at the probable full-scale Reynolds numbers of, say, between 10×10^6 and 20×10^6 , if still occurring from close to the leading edge, will be of the type analogous to the 'burst short bubble' in two-dimensional flow. In order to improve the stalling characteristics of such wings, therefore, more research is needed to determine the conditions controlling whether a bubble of the 'short' type reattaches or not and hence how the nose shape can best be designed to delay the bursting of the bubble to as high an incidence as possible. Investigation of the 'long' bubble regime is, therefore, only relevant to the study of very thin wings and of tunnel tests at low Reynolds number.

From the foregoing discussion, it appears that when more experimental evidence is available, it should be possible to correlate the rate, at which the separation extends in along the wing as the incidence is increased, with the spanwise and chordwise loadings over the wing in inviscid flow and the variation (when known) of $C_{L \text{ crit}}$ with R_t for some equivalent section in two-dimensional flow. In view of the characteristic shape of this variation (Fig. 11), the growth of the separation with increasing incidence may take crudely one of three forms, according to the free-stream Reynolds number: at low Reynolds numbers, $C_{L \text{ crit}}$ is low for all sections of the wing, except probably close to the root and so a significant separation first occurs near the tip at a relatively low incidence and extends rapidly in to near the root with only a small further increase in incidence (*e.g.*, Wing A, $R = 1.1 \times 10^6$ (Fig. 2)); at somewhat higher Reynolds numbers (*e.g.*, Wing A, $R = 3 \times 10^6$ (Fig. 1)), the values of $C_{L \text{ crit}}$ have improved over the inboard but not over the outboard parts of the wing and so the separation first occurs at almost as low an incidence as in the first case but then extends in more gradually; third, at higher Reynolds numbers still (*e.g.*, Wing A, $R = 5.7 \times 10^6$ (Fig. 2)), $C_{L \text{ crit}}$ achieves its higher value over most of the span, a significant area of separation does not occur until a much higher incidence but its inward extension with further increase of incidence is again relatively rapid. These characteristics do not, of course, change abruptly with variation in Reynolds number but gradually merge from one type to the next.

Figs. 1 and 2 illustrate that the flow patterns are influenced by changes in Reynolds numbers in other ways, apart from this effect on the rate of spanwise extension of the area of separation. For example, in the lowest Reynolds-number range, typified by the results for $R = 1.1 \times 10^6$, as already noted, the vortex sheet appears to lie initially* more closely parallel to the leading edge of the wing than is usual. This is a particularly significant observation because in the absence of any three-dimensional effects, if a long bubble formed at a relatively low C_L , it would be expected to extend rearward relatively slowly with increasing incidence. In this respect, therefore, there appears to be some connection between the three-dimensional flow pattern and what might be expected simply from two-dimensional concepts. An inspection of all the available evidence has led to the following statistical conclusion: The vortex sheet lies at its usual angle of about 20 deg to the free stream in all cases for which a turbulent reattachment would not be expected to occur in the region outboard and ahead (in a free-stream sense) of a vortex sheet lying in this direction; in other cases, as in the low Reynolds-number example cited above, the vortex sheet lies closer to the wing leading edge. It must be emphasized that this is at present merely a statistical deduction from the observed flow patterns but the fact that this limited

* *i.e.*, for incidences a little greater than that at which the vortex sheet first appears.

interrelation appears to exist raises again the question as to what is the source of the observed vorticity. As suggested in Ref. 2, various different types of vortex sheet may be present in the flow after a leading-edge separation has occurred over part of the wing, *e.g.*, the vortex sheet on top of the bubble and a part-span vortex sheet originating from the inner end of the separation near the leading edge and resulting from the difference in velocities at the boundary between the separated and unseparated regions. Ref. 2 points out that a part-span vortex sheet of the latter type would not be expected to lie in the free-stream direction but would be diverted outward, relative to this direction in the manner shown in the photographs. It has also been suggested by various authors that the vortex sheet above the bubble may roll up under the influence of the cross-flow on the swept-back wing. The available but inadequate evidence suggests that possibly both types of vortex sheet may contribute to the final observed effect. The interrelation noted above suggests that the nature of the outboard separation and hence of the vortex sheet above it has some influence. On the other hand, the fact that when the inward extension of the region of separation is arrested, *e.g.*, at the wing root or by a fence¹ (*see* Section 5), the vortex sheet usually remains located across the wing in about the same position as the incidence is increased further, thus effectively limiting any further rearward extension of the dead-air region on the sections cut by the vortex sheet strongly suggests that a part-span vortex sheet of the second type is involved.

Despite this uncertainty regarding the precise nature of the origin of the vorticity, it is convenient to continue to think in terms of a dead-air region with a part-span vortex sheet originating from its inner end and lying out across the wing rather than in terms of a separation bubble with some vorticity in the rear part of it. The first conception emphasizes the basic dissimilarity between the swept wing and two-dimensional flows and conveys a clearer picture of the shape of the chordwise pressure distributions across affected sections. Pressure-plotting tests have been made on Wing C in its unmodified state and these results (and those on other wings tested elsewhere) have shown that after separation has occurred on a given section, the suction near the leading edge cease to increase with incidence and tend to fall. A localized peak is often still maintained near the leading edge (particularly for wings of relatively high leading-edge sweep) but there is little subsequent chordwise variation in the surface pressure in the substantially dead-air region ahead of the vortex sheet. The relatively constant suction in this region is greater than that to be expected in two-dimensional flow with a separation bubble extending back to where streamwise flow is again established behind the vortex sheet. In the vicinity of the vortex sheet, the suction is increased considerably above the constant level applying further forward; this is reflected in the rapid oil scouring shown by the black areas in the photographs. The flow patterns also faithfully record that the influence of the vortex sheet on the surface pressure distributions is greatest well forward on the wing, *i.e.*, just outboard of the inner end of the separation. This should not be taken as implying that the vorticity is mostly concentrated there. In fact, the measurements in Ref. 3 showed that in at least that particular case, the vorticity increased linearly from near the leading edge back to the trailing edge but as previously pointed out, as the distance from the leading edge increases, the 'core' of the vorticity occurs further out from the wing surface.

3.2.1. *Flow patterns outboard of the vortex sheet.*—Little has so far been said about the oil-flow patterns outboard of the vortex sheet beyond noting that even in those cases where the oil does flow over this region, the rate at which it flows is extremely small, thus indicating that there is little airflow close to the surface. This is perhaps the most that can be deduced with certainty but, nevertheless, it is possible to distinguish between two different types of oil behaviour outboard of the vortex sheet, as can be seen, for example, by comparing the patterns for Wings A and B at high incidence in Fig. 3. In the case of Wing B, the oil-flow lines, outboard of the vortex sheet, turn towards the free-stream direction and then coalesce into one 'river' of oil which flows off the trailing edge, outboard of the sheet. Outboard of this, the pattern preserves its original mottled appearance, *i.e.*, the titanium oxide suspension remains in its original state, except for a band round the leading edge in which there is relatively rapid flow, almost parallel to the leading

edge but slightly from the lower surface round to the upper surface. With Wing A, these effects are only observed, and to a lesser degree, just outboard of the vortex sheet and close to the leading edge. Over most of the chord, the oil-flow lines first turn towards the free-stream direction, as the component of velocity, owing to the vortex sheet, decreases but then they run spanwise, then forward to near the leading edge and finally the oil runs down the leading edge towards the origin of the vortex sheet*. The latter behaviour is similar to what was observed by Black⁵ in his experiments. Statistically, on the present evidence, it appears that the wing plan-form is the most important parameter governing which type of oil pattern is observed. The second type is usually obtained when the sweepback of the part of the wing affected is 40 deg or less while the first type is obtained with the wings of higher sweep. It is perhaps more correct to say that the second type is usually obtained when an appreciable proportion of the span lies outboard of the influence of the vortex sheet and the first type when this is not so. In Ref. 3, it is suggested that the first type when the oil piles up and coalesces into one river marking the inner boundary of the dead-air region occurs when the boundary layer of the spanwise flow under the vortex sheet separates as a result of the adverse pressure gradient beyond the sheet. On this reasoning, the second type, obtained with the 40 deg swept wings, occurs when this boundary layer does not separate. This reasoning appears quite plausible, for this second type is observed in those cases in which it might be expected that the adverse pressure gradient opposing this flow just outboard of the sheet would be relatively small. This follows because the suction over the rear of the outer sections would be increased considerably since the flow over them had fully separated back to the trailing edge and hence might be comparable with the suction close to the surface in the vicinity of the vortex sheet (bearing in mind that under these conditions, the main part of the sheet would be some distance away from the surface).

It is thought that the actual flow pattern obtained with the oil over the dead-air region of the less swept wings is dictated by the pressure distribution over the wing surface in that the slowly moving oil always tends to seek a position where the suction is greater. On this basis, it would appear that there is a small pressure recovery back to the trailing edge in the fully separated region. This is also observed in two-dimensional flow after a 'short' bubble has burst.

The characteristic of oil flowing almost along the leading edge from the lower surface round to the upper surface is certainly dependent on the wing plan-form and as might be expected, it becomes more pronounced as the angle of sweepback of the leading edge is increased. It may be stressed that the characteristic is only evident after the flow has separated over the upper surface, *i.e.*, after the collapse of the peak suction very close to the leading edge.

3.2.2. *Flow Patterns Inboard of the Vortex Sheet.*—One other characteristic deserving of mention is observed in the flow patterns at high Reynolds numbers, *i.e.*, when the separation does not extend in from the tip until a relatively high incidence is reached. It can be seen in the photographs for Wing B at $R = 6 \times 10^6$ (Fig. 4). If it is assumed, as previously, that the projection of the vortex sheet in the wing surface is a line inclined at about 20 deg to the free-stream direction and originating near the leading edge near the inner end of the separation, then, inboard of this line, the oil does not flow in a smooth, orderly fashion across the wing. Instead, the oil flows back from the leading edge but at about $0.1c$, turns outward in a roughly spanwise direction and flows towards what has been defined as the origin of the vortex sheet. There is a clear division between the oil flow that behaves in this way and the flow behind, which is behaving as would be expected with the flow direction rearward but with a considerable spanwise component owing to the spanwise drift in the sub-layer of the boundary layer (and the flow through the gap in the wing-body junction). The relatively black area in such final photographs as that for Wing B, $\alpha = 15$ deg, $R = 6 \times 10^6$ (Fig. 4), indicates the region into which the oil flows rapidly after the tunnel is started. It will be seen that the area is broader at its inner end and is crudely focussed at the point on the leading edge marking the inner end of the separation.

* The oil which creates this pattern comes from further inboard; the titanium oxide suspension originally put on this part of the wing is again unaffected and forms a background to the superimposed pattern.

The explanation of this characteristic is not known but it is suggested tentatively that it does not indicate the existence of any flow separation in this vicinity but possibly an area in which the chordwise pressure gradient is relatively slight but in which there is a marked spanwise pressure gradient, *i.e.*, that it is another example of the oil seeking a point where the suction is greater. This suggestion is certainly in accord with expectation as regards the pressure distributions over the wing surface, even to the extent of suggesting that at a given incidence, the region in which the pressure varies relatively little in a chordwise direction decreases with distance out along the span.

The greatly increased spanwise drift in the lower part of the boundary layer at high incidences may also contribute to the observed effect.

4. *Typical Effects on Overall Forces and Moments.*—It is not the purpose of this paper to comment in detail on how the overall forces and moments are affected by the flow characteristics just described. Some brief notes are, however, pertinent.

The only definite prediction that can be made regarding the variation of the overall forces and moments with incidence following the appearance of a region of separated flow is that the rate of increase of C_D with C_L^2 should be markedly increased. Indeed, in the absence of flow photographs, it is often possible to deduce when a separation has occurred from examination of the drag data. $(\partial C_D / \partial C_L^2)$ should increase even more rapidly after the vortex sheet has ceased to restrict the rearward extension of the dead-air region.

The effects on lift and pitching moment are much more complex and cannot be easily predicted. Various opposing effects are present: for example, as a result of the separation over the forward part of the outer sections, $(\partial C_L / \partial \alpha)_M$ is reduced; the local aerodynamic centre for these outer sections moves rearward; on the other hand, as the reduction in lift occurs aft of the aerodynamic centre for the wing as a whole, the change in spanwise loading tends to reduce $(-\partial C_m / \partial C_L)_M$. Also, as a result of the presence of the part-span vortex sheet, the overall $(\partial C_L / \partial \alpha)_M$ is increased; the local aerodynamic centre of the sections cut by the vortex sheet can move rearward or forward according to the position of the sheet along the chord and the effects of the vortex sheet on the spanwise loading tends to give an increase in $(-\partial C_m / \partial C_L)_M$ when the vortex sheet is far out on the wing and to decrease it when the origin of the sheet is close to the wing root (the main effect of the vortex sheet being to increase the lift just inboard of the sheet). The balance between all these factors varies from one wing to another and with incidence for any given wing. The following conclusions generally apply, however, for wings of 'simple' design (*see* Section 2):

- (i) In the incidence range immediately after the first appearance of a leading edge separation near the tip, the 'end-plate' effects of the vortex sheet will predominate, giving an increase in both $(\partial C_L / \partial \alpha)_M$ and $(-\partial C_m / \partial C_L)_M$.
- (ii) As the incidence is increased further $(\partial C_L / \partial \alpha)_M$ and $(-\partial C_m / \partial C_L)_M$ usually decrease because of the increased importance of the loss in lift over the wing outboard of the part-span vortex sheet.
- (iii) For wings with an angle of sweep of, say, 40 deg or less, if a serious reduction in $(-\partial C_m / \partial C_L)_M$ occurs at high C_L , then this is principally related to this loss in lift over the outer sections. On the other hand, for a wing with, say, 60 deg of sweep and more particularly if it is highly tapered, this loss in lift is not so severe because a part-span vortex sheet, even when originating from close to the wing root restricts the dead-air region to relatively small proportions (*e.g.*, Wing D (Fig. 5)). In the case of a highly swept wing, serious reductions in $(-\partial C_m / \partial C_L)_M$ at high C_L tend to be associated with an increase in lift over the forward part of the inner sections (because of the increase in suctions just inboard of the vortex sheet).
- (iv) The action of the part-span vortex sheet in effectively limiting over a certain incidence range, the rearward extension (in the free-stream direction) of at least part of the

substantially dead-air region, together with its 'end-plate' effect on the pressure distribution inboard of it result in an increase of the local $C_{L \max}$ of the inner sections of the wing and may even result in the overall $C_{L \max}$ being higher than for a two-dimensional wing with the same section. This effect is clearly greater for the wings of higher sweep since less of the wing then lies outboard of the influence of the part-span vortex sheet from near the root (*e.g.*, Wing A, Fig. 1) and also since the extension of a leading-edge separation completely into the wing root tends to be more delayed with the more highly swept wings. This provides the explanation of the often noted result that the value of the actual $C_{L \max}$ (as distinct from the usable $C_{L \max}$) increases with sweep to reach a maximum for angles of sweep of between 50 deg and 60 deg (This increase is not observed for relatively thick swept-back wings for which the stall is not associated with a leading-edge separation and for which, therefore, there is no strong part-span vortex sheet of the type being considered here).

It will readily be appreciated that the various non-linear effects in the overall results for a given wing should appear at lower values of C_L at low Reynolds numbers but that then, as the development of the stall is spread over a larger range of incidence than at high Reynolds numbers, the changes are more gradual than those to be expected at higher Reynolds numbers. Hence, results at low Reynolds numbers are not necessarily pessimistic; the pitch-up at high Reynolds numbers may be much more abrupt and unpleasant. The analysis of the flow patterns suggests that for wings with thickness/chord ratios of not less than 0.06, there should be little scale effect on the overall results for $R > 6 \times 10^6$ unless or until transition occurs at high incidence ahead of where the laminar boundary layer would otherwise separate and the leading-edge separation is replaced by a turbulent separation from the rear, as for thicker wings. Even then, no large quantitative change with Reynolds number may occur.

5. *Some Notes on Methods of Improving the Characteristics at High Incidence.*—From the foregoing discussion, it appears likely that the best methods for improving the longitudinal trim and stability characteristics of a swept-back-wing design at high incidence will vary between different examples. In general, it will not be sufficient to incorporate some modification, *e.g.*, to wing section shape, plan-form and/or twist, that would prevent the premature separation near the tip*. Indeed, such a modification, taken by itself, might delay any reduction in $(-\partial C_m / \partial C_L)_M$ to a higher value of C_L but only at the expense of a more severe reduction when it occurred. Crudely, in the same way as in Section 4, a distinction may be drawn between wings of about 40 to 45 deg sweep and those of, say, 60 deg sweep. With the first group, the primary aim should be to arrange that when a separation occurs (almost inevitably, near the tip) it should be allowed to extend in rapidly until it is of such a spanwise extent that the opposing effects of the separation and associated part-span vortex sheet roughly balance as regards $(-C_m / \partial C_L)_M$; the separation should then be confined to this extent up to as high an incidence as possible. With the wings of higher sweep, the primary aim should be to prevent the separation extending in to the vicinity of the wing root up to as high an incidence as possible, thus preventing the nose-up moment from an increase in lift well ahead of the wing aerodynamic centre. Examples of both can be found in the present collection of designs:

(i) *Modifications to Control the Outer Separation.*—Fences and leading-edge chord extensions are examples of modifications that derive their principal benefit not from delaying the first appearance of a separation but from controlling its subsequent growth (*see* Ref. 1). For example, the photographs in Fig. 8 for Wing C with a fence fitted at $0.56 \times$ semi-span indicate that, as near the wing root, separation near the leading edge just outboard of the fence is delayed to a higher incidence by the presence of the fence; a part-span vortex sheet continues to originate from just outboard of the fence and so the dead-air region near the leading edge of the outer

* The ability to calculate the pressure distributions over the entire wing surface at high incidence is probably not good enough, in any case, to achieve any academic aim such as arranging for the separation to occur at the same incidence at different stations along the span.

sections is considerably restricted (*cf.* the photographs for the wing with and without fence for $\alpha = 16$ deg (Fig. 8)). For this particular wing, a reduction in stability still occurs even with the fence, when the part-span vortex sheet outboard of the fence effectively or literally lifts off the wing surface, but there is a gain of about 0.2 in the value of C_L for the reduction in stability, compared with the results for the wing without fence. For a less swept wing, the redistribution of the area of separation (being less, outboard and greater, inboard of the fence) might be sufficient for the reduction in stability to be prevented altogether.

Even better results should be possible with a modification that both delays the appearance of a separation near the leading edge near the tip and also controls the development of the separation. An example of this is the modification, tested with Wing C, incorporating the drooped-nose shape shown in Fig. 10 over the part of the wing outboard of $0.56 \times$ semi-span. The photographs in Fig. 9 show that with this modification at $R = 3 \times 10^6$, the flow does not separate near the leading edge of the drooped part of the wing until beyond $\alpha = 20$ deg, compared with $\alpha = 8$ deg for the start of the separation near the tip of the original wing at this Reynolds number. Because of the discontinuity in the leading edge at $0.56 \times$ semi-span, the separation near the leading edge inboard of here is induced at a lower incidence than for the original wing and part-span vortex sheets originate from near both the inner and outer ends of this separation and off the discontinuity itself. It is thought that these help to prevent a turbulent separation from the rear of the outer drooped sections, which might otherwise occur at some incidence in the range of improvement from $\alpha = 8$ deg to $\alpha = 20$ deg. The particular, rather complex flow patterns obtained in this case are such that the C_m against C_L curve is reasonably linear up to beyond $C_L = 1.0$ ($\alpha = 20$ deg). It was found that further improvements could be obtained by adding a fence over the rear part of the section at $0.56 \times$ semi-span.

With highly tapered, relatively thin wings, the various opposing effects on C_L and C_m , resulting from the separation over the outer sections and the associated part-span vortex sheet tend to balance out even if no special modification is included; at least, until the separation has extended fairly close to the root. This point is illustrated by the results for Wing D: the reduction in stability at the test Reynolds number of $R = 2.7 \times 10^6$ does not occur until $\alpha = 11$ deg, whereas the flow has separated from near the leading edge near the tip from about $\alpha = 2$ deg (Fig. 5).

(ii) *Modifications at the Root of Highly Swept Wings.*—No data are included in the present paper which directly indicate what can be achieved in this way. Improvements in the overall characteristics of several of the wings considered have been obtained, however, by means of some change that prevents, over a certain range of incidence, the inward movement of the inner end of the separation beyond a certain position along the span. Two examples are as follows: First, the magnitude of the reduction in stability at high C_L with Wing B was considerably alleviated by the addition to the model of a wing-root leading-edge intake fairing and second, the results for Wing E were considerably improved by the addition of a drooped-nose flap extending from the wing root out to about $0.41 \times$ semi-span. In the latter case, the improvement was most marked for Mach numbers near $M = 0.85$ to 0.90 but the basic nature of the flow characteristics is then still similar to that at low Mach number.

A similar sort of delaying action is needed to improve the overall characteristics of Wing D for which a significant nose-up moment change has been observed above about $\alpha = 15$ deg in tests in another tunnel at about $R = 2.7 \times 10^6$. In this case, the wing-root intake fairing is not effective in the same way as for Wing B; indeed, its effect is probably harmful because, as can be seen from the photographs in Fig. 5, a vortex sheet associated with a separation over the sharp upper lips of this intake fairing occurs at a relatively low incidence ($\alpha = 8.4$ deg). From this aspect, it would be preferable to round the lips of the intake but even then, some form of fence or discontinuity in the wing leading edge, outboard of the intake, might be required.

6. *Concluding Remarks.*—It is hoped that this collection of flow patterns over different wings and the accompanying discussion has helped in appreciating the various factors that determine

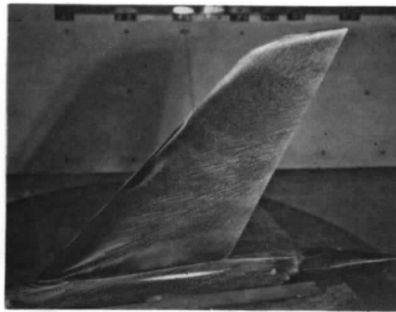
the overall force and moment characteristics at high incidence for swept-back wings that suffer from a leading-edge separation, and so in understanding what sort of modifications may prove effective in improving these characteristics in specific cases. It will have been realized that understanding of even the flow patterns themselves is not complete and more experimental evidence is required.

The discussion suggests that some form of correlation may ultimately be established between the flow over two-dimensional and over three-dimensional swept-back wings as regards the values of C_L at which the flow first separates (and hence, as regards the spanwise extent of the separation over the swept wing at a given incidence). It is interesting to note that for the probable flight Reynolds numbers, if the separation is still of the leading edge type, it should be analogous to the 'burst short bubble' case in two-dimensional flow for wings with thickness/chord ratios of 0.06 or more and probably for some thinner wings as well.

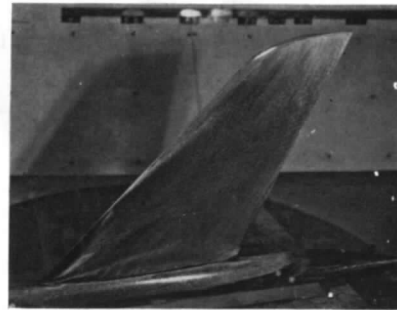
No correlation can be expected regarding the growth with incidence of the chordwise extent of the separation in two-dimensional and three-dimensional flow in view of the effects of a (possibly rolled-up) vortex sheet lying inboard and to the rear of the substantially dead-air region over the surface of the swept-back wings. Conclusions regarding the position and characteristics of this vortex sheet are still largely on an empirical basis and more research is needed to understand them more soundly.

REFERENCES

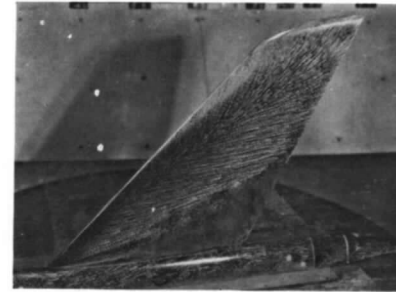
- | <i>No.</i> | <i>Author</i> | <i>Title, etc.</i> |
|------------|----------------------------------|--|
| 1 | A. B. Haines and C. W. Rhodes .. | Tests in the R.A.E. 10-ft \times 7-ft High Speed Tunnel on three wings with 50-deg sweepback and 7.5 per cent thick sections. R. & M. 3043. September, 1954. |
| 2 | D. Kuchemann | Types of flow on swept wings with special reference to free boundaries and vortex sheets. A.R.C. 15,756. March, 1953. Also <i>J. R. Ae. Soc.</i> , November, 1953. |
| 3 | T. Ornberg | A note on the flow around delta wings. K.T.H. Aero. Tech. Note 38, February, 1954. Reproduced in part as A.R.C. 16,795. May, 1954. |
| 4 | P. R. Owen and L. Klanfer .. | On the laminar boundary-layer separation from the leading edge of a thin aerofoil. A.R.C. 16,576. November, 1953. |
| 5 | J. Black | A note on the vortex patterns in the boundary-layer flow of a swept-back wing. <i>J. R. Ae. Soc.</i> April, 1952. |



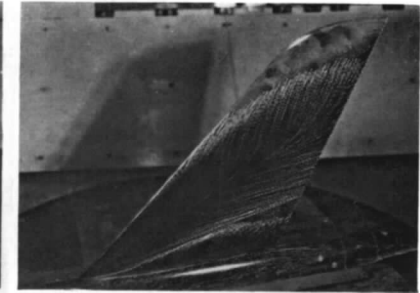
$\alpha = 8 \text{ deg}, C_L = 0.50$



$\alpha = 9 \text{ deg}, C_L = 0.59$

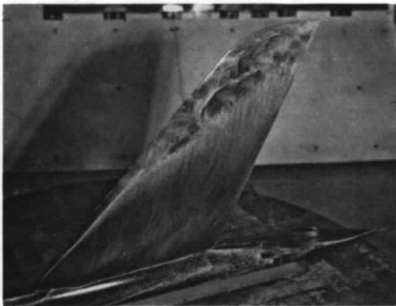


$\alpha = 8 \text{ deg}, C_L = 0.53$

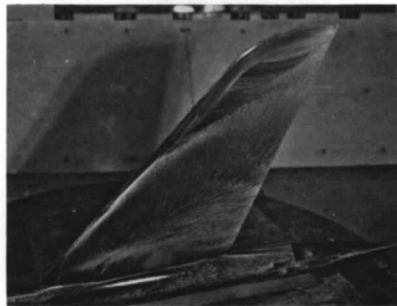


$\alpha = 10 \text{ deg}, C_L = 0.66$

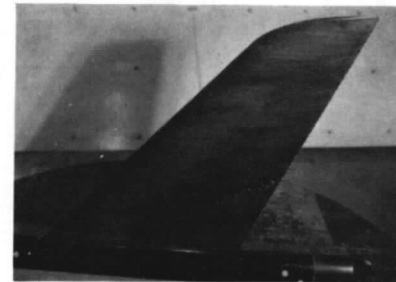
$R = 1.1 \times 10^6 (M = 0.33)$



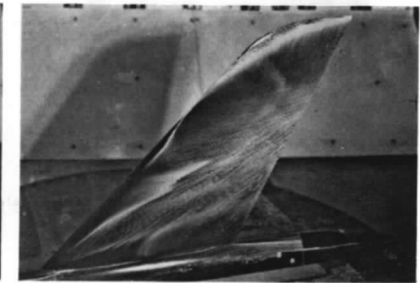
$\alpha = 10 \text{ deg}, C_L = 0.66$



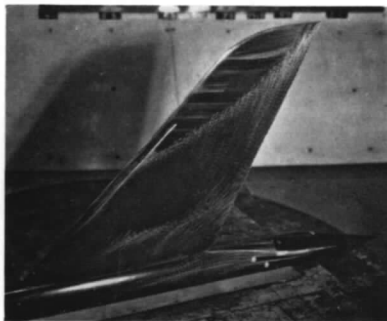
$\alpha = 13 \text{ deg}, C_L = 0.81$



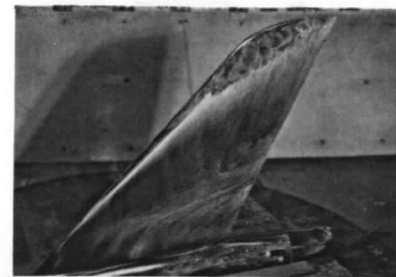
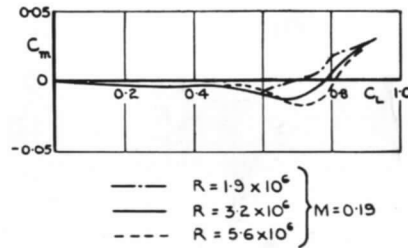
$\alpha = 10 \text{ deg}, C_L = 0.65$



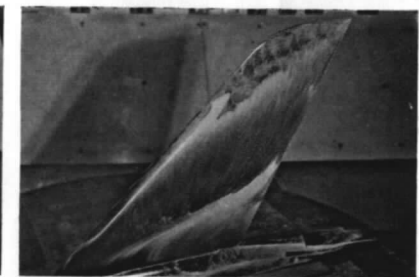
$\alpha = 12 \text{ deg}, C_L = 0.77$



$\alpha = 16 \text{ deg}, C_L = 0.89$



$\alpha = 14 \text{ deg}, C_L = 0.88$



$\alpha = 16 \text{ deg}, C_L = 0.91$

$R = 5.7 \times 10^6 (M = 0.19)$

FIG. 1. Flow patterns for Wing A: $R = 3 \times 10^6 (M = 0.27_3)$
 $(t/c = 0.06; \phi_{0.25c} = 40 \text{ deg})$.

FIG. 2. Effect of Reynolds number on flow patterns for Wing A
 (See FIG. 1 for intermediate Reynolds number and C_m vs. C_L curves).

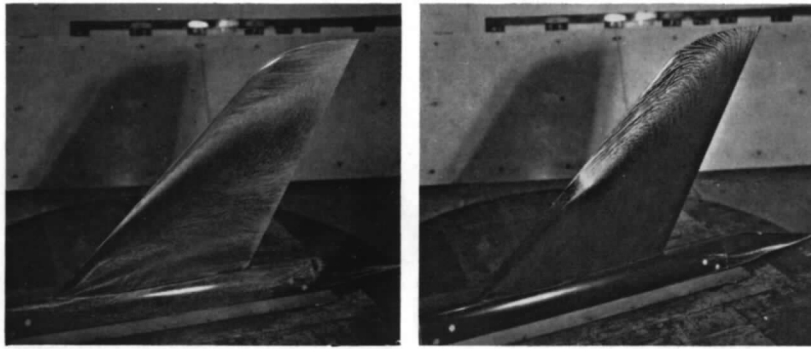


Fig. 3(a) Wing A, $\bar{\alpha} = 18$ deg, $C_L = 0.93$, $R = 3 \times 10^6$

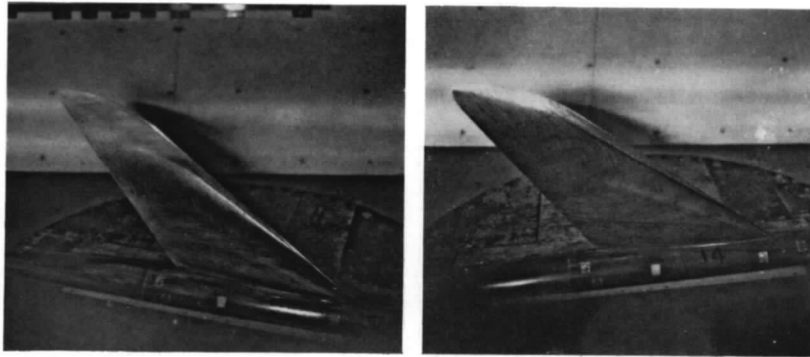


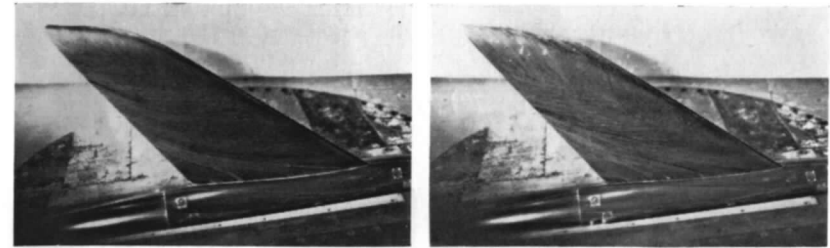
Fig. 3(b) Wing B, $\alpha = 14$ deg, $C_L = 0.85$, $R = 2.5 \times 10^6$

18

Photographs on left taken soon after starting tunnel

Photographs on right taken after oil has dried

FIGS. 3a and 3b. Comparison of 'early' and 'final' flow patterns for Wings A and B.

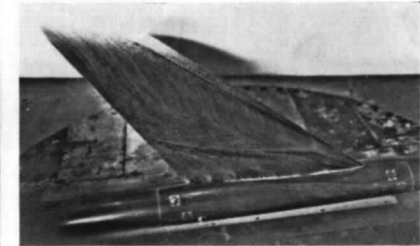


$\alpha = 8$ deg, $C_L = 0.50$

$\alpha = 10$ deg, $C_L = 0.63$



$\alpha = 12$ deg, $C_L = 0.75$



$\alpha = 14$ deg, $C_L = 0.85$

$R = 2.5 \times 10^6$



$\alpha = 15$ deg, $C_L = 0.90$



$\alpha = 18$ deg, $C_L = 1.01$

$R = 6 \times 10^6$

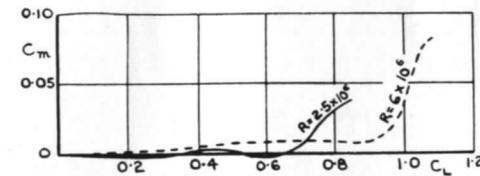
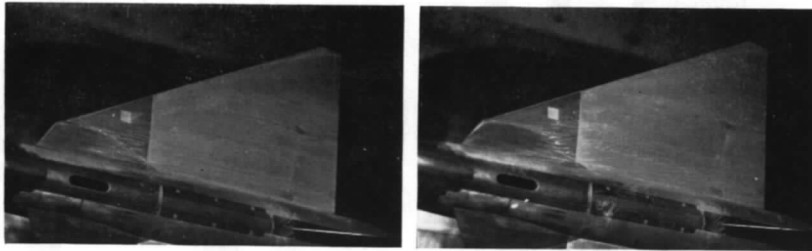
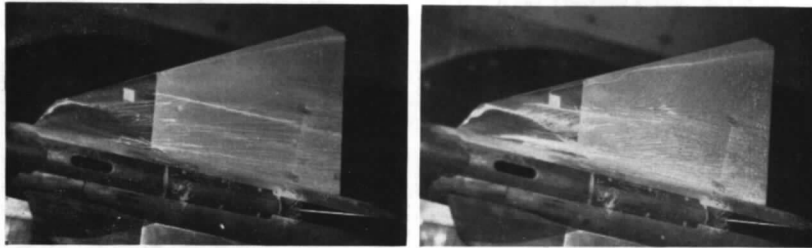


FIG. 4. Effect of Reynolds number on flow patterns for Wing B ($t/c = 0.075$; $\phi_{0.25c} = 48.6$ deg).



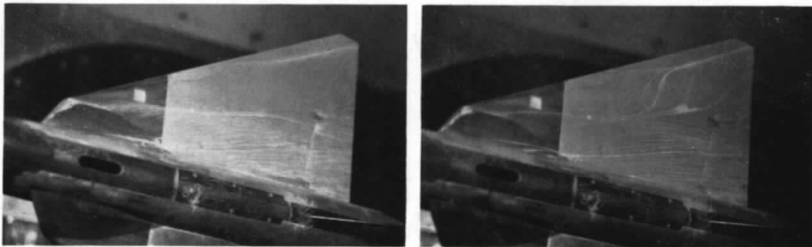
$\alpha = 4.2 \text{ deg}, C_L = 0.16$

$\alpha = 6.3 \text{ deg}, C_L = 0.25$



$\alpha = 8.4 \text{ deg}, C_L = 0.34$

$\alpha = 10.5 \text{ deg}, C_L = 0.45$



$\alpha = 11.6 \text{ deg}, C_L = 0.50$

$\alpha = 12.6 \text{ deg}, C_L = 0.55$

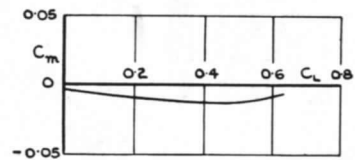
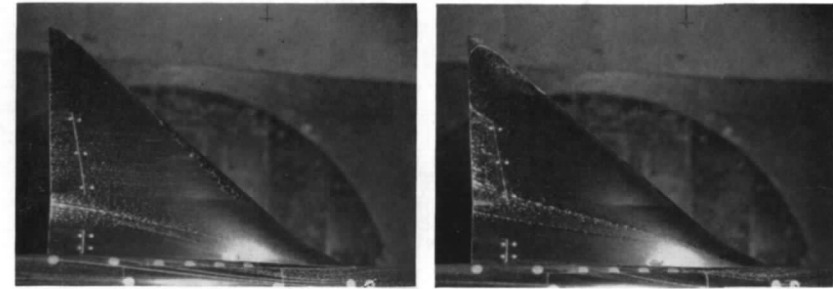
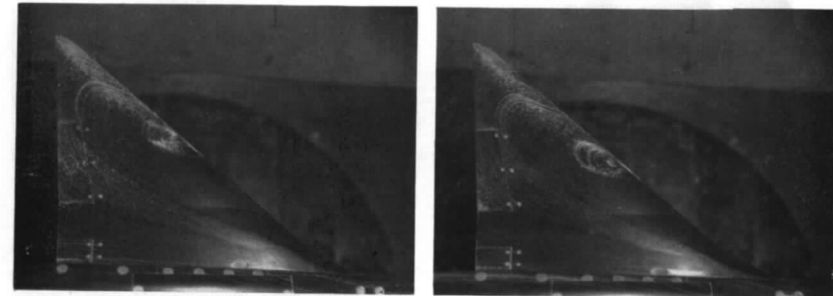


FIG. 5. Flow patterns for Wing D, $R = 2.7 \times 10^6$
($t/c = 0.04$; $\phi_{L.E.} = 60 \text{ deg}$).



$\alpha = 6.3 \text{ deg}, C_L = 0.27$

$\alpha = 10.5 \text{ deg}, C_L = 0.49$



$\alpha = 14.8 \text{ deg}, C_L = 0.68$

$\alpha = 15.8 \text{ deg}, C_L = 0.72$

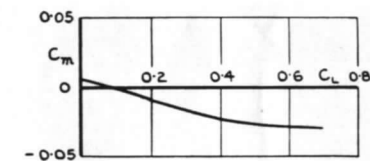
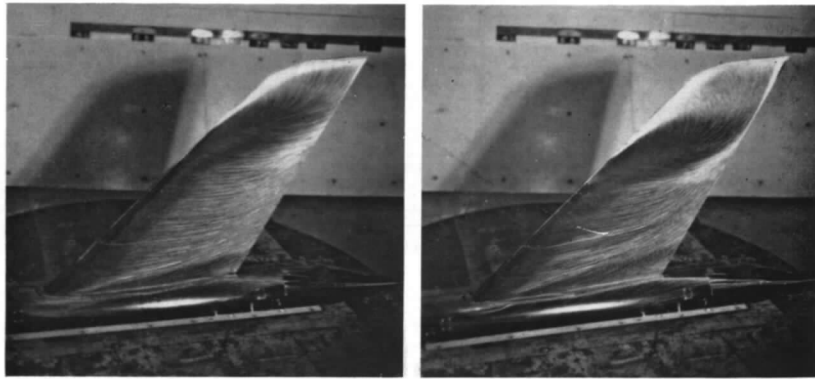
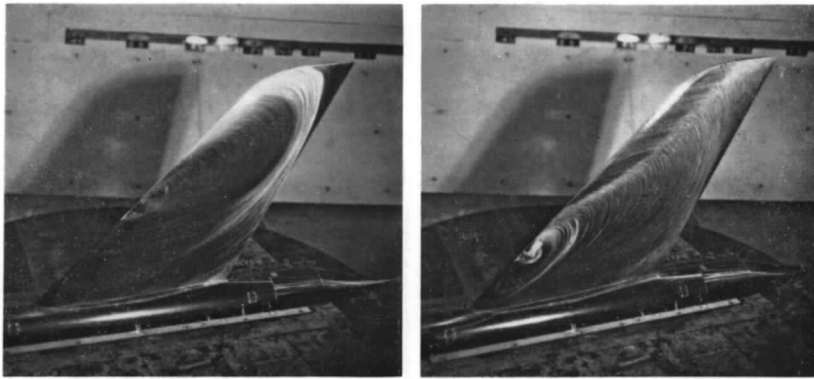


FIG. 6. Flow patterns for Wing E, $R = 2.3 \times 10^6$
(t/c varying from 0.135_{root} to 0.08_{tip} ; $\phi_{L.E.} = 49.9 \text{ deg}$).



$\alpha = 10 \text{ deg}, C_L = 0.63$

$\alpha = 12 \text{ deg}, C_L = 0.75$



$\alpha = 14 \text{ deg}, C_L = 0.84$

$\alpha = 18 \text{ deg}, C_L = 0.92$

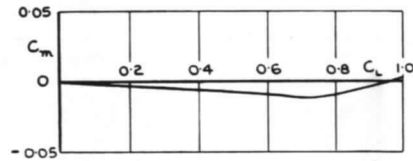
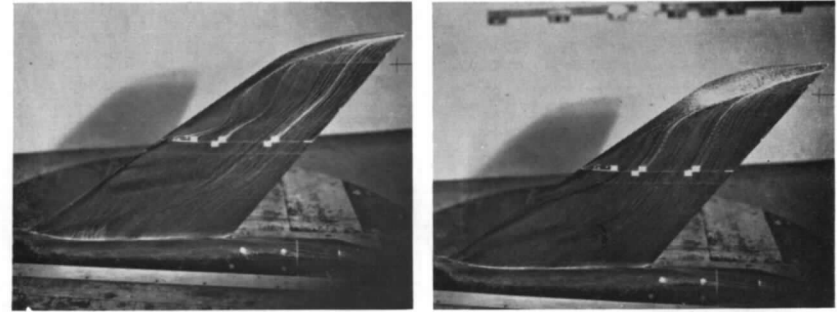


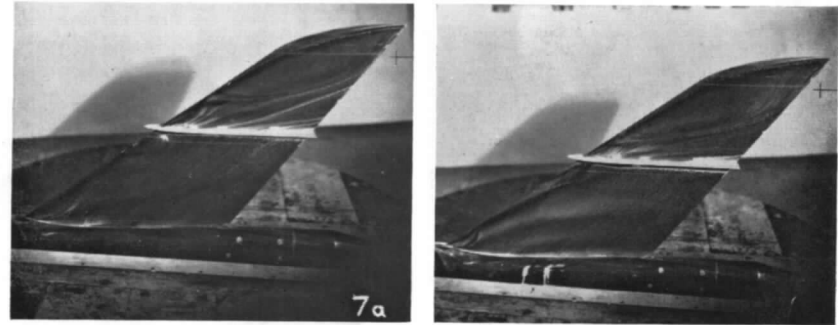
FIG. 7. Flow patterns for Wing F, $R = 2.0 \times 10^6$
($t/c = 0.10$; $\phi_{0.25c} = 40 \text{ deg}$; section shape varying along span).



$\alpha = 14 \text{ deg}, C_L = 0.84$

$\alpha = 16 \text{ deg}, C_L = 0.94$

Wing K in unmodified form



$\alpha = 14 \text{ deg}, C_L = 0.85$

$\alpha = 16 \text{ deg}, C_L = 0.95$

Wing K with fence at $0.56 \times$ semi-span

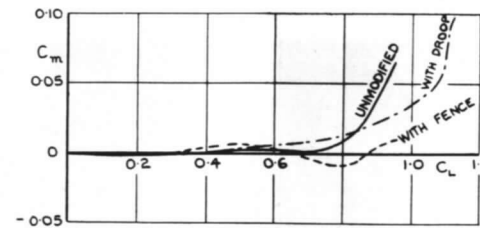
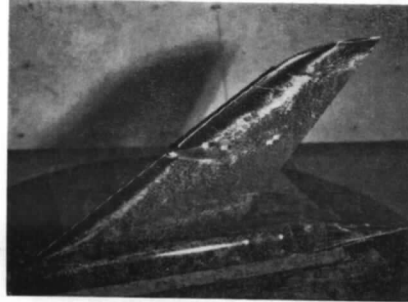
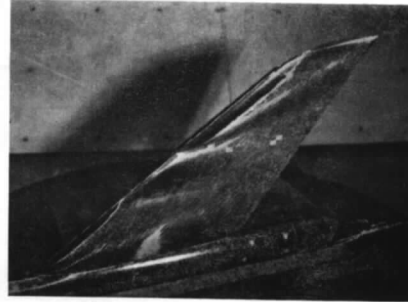


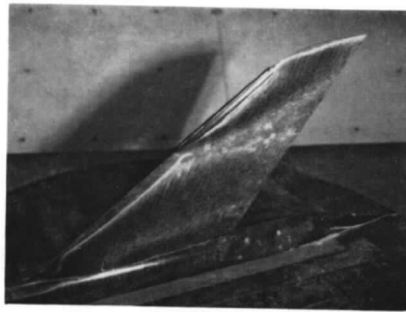
FIG. 8. Effect of fence on flow patterns for Wing C, $R = 2.7 \times 10^6$
($t/c = 0.075$; $\phi_{0.25c} = 50 \text{ deg}$).



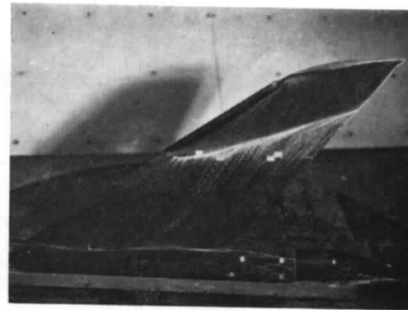
$\alpha = 10 \text{ deg}, C_L = 0.61$



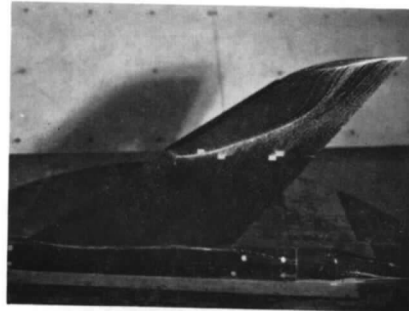
$\alpha = 14 \text{ deg}, C_L = 0.83$



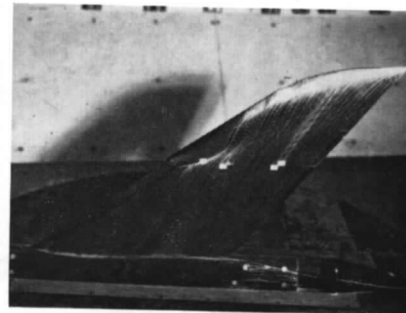
'Early' Photograph $\alpha = 18 \text{ deg}, C_L = 1.01$



'Late' Photograph



$\alpha = 20 \text{ deg}, C_L = 1.07$



$\alpha = 22 \text{ deg}, C_L = 1.14$

For C_m vs. C_L curve, see Fig. 12; Droop Shape, see Fig. 14.

FIG. 9. Flow patterns for Wing C with drooped nose from 0.56 to $0.88 \times$ semi-span ($R = 2.7 \times 10^6$).

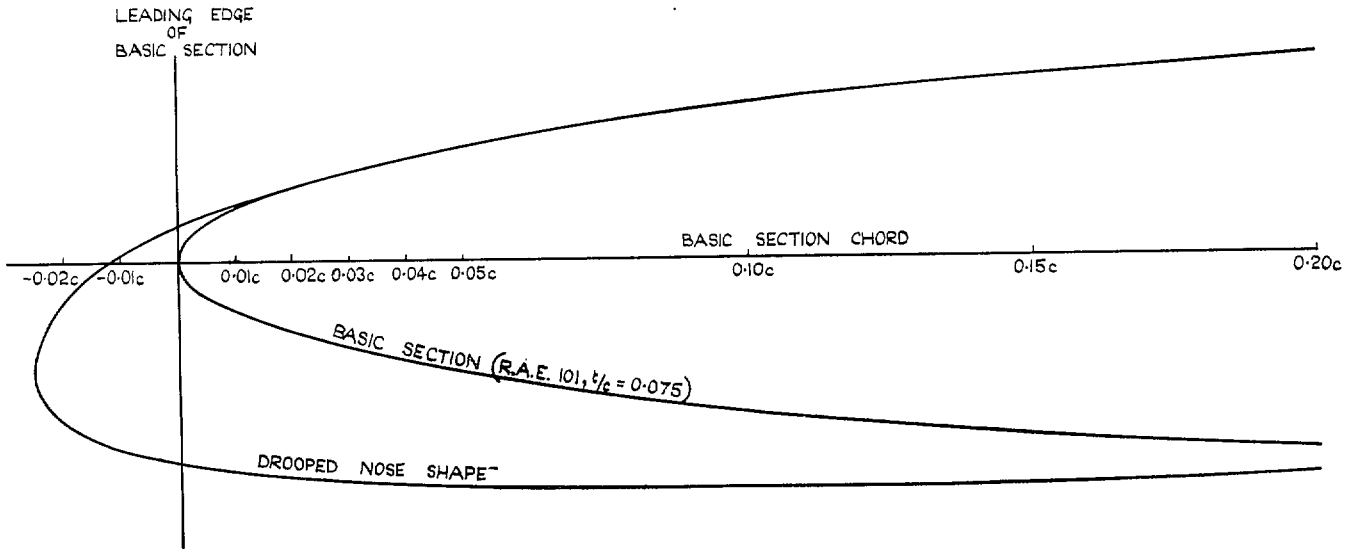
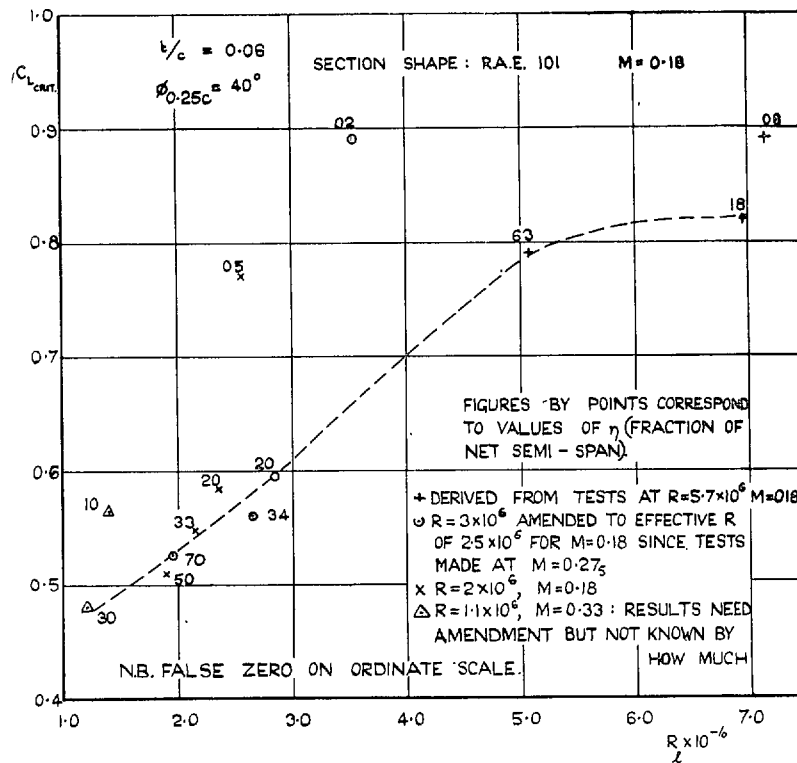


FIG. 10. Shape of drooped nose fitted to Wing C outboard of $\eta = 0.56$ (Gross semi-span).



$C_{L,crit}$ = APPROXIMATE VALUE OF LOCAL C_L AT WHICH FLOW FIRST SEPARATES.

FIG. 11. Variation of $C_{L,crit}$ with local Reynolds number (R_l) for Wing A.

Publication of the Aeronautical Research Council

ANNUAL TECHNICAL REPORTS OF THE AERONAUTICAL RESEARCH COUNCIL (BOUND VOLUMES)

- 1939 Vol. I. Aerodynamics General, Performance, Airscrews, Engines. 50s. (52s.)
Vol. II. Stability and Control, Flutter and Vibration, Instruments, Structures, Sea-planes, etc. 63s. (65s.)
- 1940 Aero and Hydrodynamics, Aerofoils, Airscrews, Engines, Flutter, Icing, Stability and Control, Structures, and a miscellaneous section. 50s. (52s.)
- 1941 Aero and Hydrodynamics, Aerofoils, Airscrews, Engines, Flutter, Stability and Control, Structures. 63s. (65s.)
- 1942 Vol. I. Aero and Hydrodynamics, Aerofoils, Airscrews, Engines. 75s. (77s.)
Vol. II. Noise, Parachutes, Stability and Control, Structures, Vibration, Wind Tunnels. 47s. 6d. (49s. 6d.)
- 1943 Vol. I. Aerodynamics, Aerofoils, Airscrews. 80s. (82s.)
Vol. II. Engines, Flutter, Materials, Parachutes, Performance, Stability and Control, Structures. 90s. (92s. 9d.)
- 1944 Vol. I. Aero and Hydrodynamics, Aerofoils, Aircraft, Airscrews, Controls. 84s. (86s. 6d.)
Vol. II. Flutter and Vibration, Materials, Miscellaneous, Navigation, Parachutes, Performance, Plates and Panels, Stability, Structures, Test Equipment, Wind Tunnels. 84s. (86s. 6d.)
- 1945 Vol. I. Aero and Hydrodynamics, Aerofoils. 130s. (132s. 9d.)
Vol. II. Aircraft, Airscrews, Controls. 130s. (132s. 9d.)
Vol. III. Flutter and Vibration, Instruments, Miscellaneous, Parachutes, Plates and Panels, Propulsion. 130s. (132s. 6d.)
Vol. IV. Stability, Structures, Wind Tunnels, Wind Tunnel Technique. 130s. (132s. 6d.)

Annual Reports of the Aeronautical Research Council—

1937 2s. (2s. 2d.) 1938 1s. 6d. (1s. 8d.) 1939-48 3s. (3s. 5d.)

Index to all Reports and Memoranda published in the Annual Technical Reports, and separately—

April, 1950 - - - - R. & M. 2600 2s. 6d. (2s. 10d.)

Author Index to all Reports and Memoranda of the Aeronautical Research Council—

1909—January, 1954 R. & M. No. 2570 15s. (15s. 8d.)

Indexes to the Technical Reports of the Aeronautical Research Council—

December 1, 1936—June 30, 1939	R. & M. No. 1850 1s. 3d. (1s. 5d.)
July 1, 1939—June 30, 1945	R. & M. No. 1950 1s. (1s. 2d.)
July 1, 1945—June 30, 1946	R. & M. No. 2050 1s. (1s. 2d.)
July 1, 1946—December 31, 1946	R. & M. No. 2150 1s. 3d. (1s. 5d.)
January 1, 1947—June 30, 1947	R. & M. No. 2250 1s. 3d. (1s. 5d.)

Published Reports and Memoranda of the Aeronautical Research Council—

Between Nos. 2251-2349	R. & M. No. 2350 1s. 9d. (1s. 11d.)
Between Nos. 2351-2449	R. & M. No. 2450 2s. (2s. 2d.)
Between Nos. 2451-2549	R. & M. No. 2550 2s. 6d. (2s. 10d.)
Between Nos. 2551-2649	R. & M. No. 2650 2s. 6d. (2s. 10d.)
Between Nos. 2651-2749	R. & M. No. 2750 2s. 6d. (2s. 10d.)

Prices in brackets include postage

HER MAJESTY'S STATIONERY OFFICE

York House, Kingsway, London W.C.2; 423 Oxford Street, London W.1; 13a Castle Street, Edinburgh 2;
39 King Street, Manchester 2; 2 Edmund Street, Birmingham 3; 109 St. Mary Street, Cardiff;
Tower Lane, Bristol, 1; 80 Chichester Street, Belfast, or through any bookseller.